

# Goal Recognition using Actor-Critic Optimization

Ben Nageris<sup>1</sup>, Felipe Meneguzzi<sup>2</sup>, Reuth Mirsky<sup>1,3</sup>

<sup>1</sup>Bar Ilan University, Israel

<sup>2</sup>University of Aberdeen, Scotland, UK

<sup>3</sup>Tufts University, MA, USA

benabraham.nageris@live.biu.ac.il, felipe.meneguzzi@abdn.ac.uk, reuth.mirsky@tufts.edu

## Abstract

Goal Recognition aims to infer an agent’s goal from a sequence of observations. Existing approaches often rely on manually engineered domains and discrete representations. Deep Recognition using Actor-Critic Optimization (DRACO) is a novel approach based on deep reinforcement learning that overcomes these limitations by providing two key contributions. First, it is the first goal recognition algorithm that learns a set of policy networks from unstructured data and uses them for inference. Second, DRACO introduces new metrics for assessing goal hypotheses through continuous policy representations. DRACO achieves state-of-the-art performance for goal recognition in discrete settings while not using the structured inputs used by existing approaches. Moreover, it outperforms these approaches in more challenging, continuous settings at substantially reduced costs in both computing and memory. Together, these results showcase the robustness of the new algorithm, bridging traditional goal recognition and deep reinforcement learning.

## 1 Introduction

Goal recognition (GR) is a fundamental problem in AI where the objective is to infer the terminal goal of an observed agent from a sequence of observations (Sukthankar et al. 2014). GR techniques can be used for estimating people’s paths (Vered and Kaminka 2017), recognizing actions in a kitchen for a service robot to fetch the required ingredients (Kautz, Allen et al. 1986; Shvo et al. 2022), or even alerting an operator when a client executes a suspicious sequence of actions in e-commerce software (Qin and Lee 2004). A recognition task contrasts a sequence of observations, represented as discrete, symbolic actions, with a domain theory that describes the domain’s possible actions to infer the likely goal from the observations. This process inherits three fundamental limitations of using a symbolic domain theory. First, using such domain theories forces the recognizer to rely on accurate and relevant symbols and limits the size of feasible problems. Second, these underlying models often represent an optimal plan for a goal but require additional extensions to handle noise in the recognition process. Third, recognizing goals in continuous domains neces-

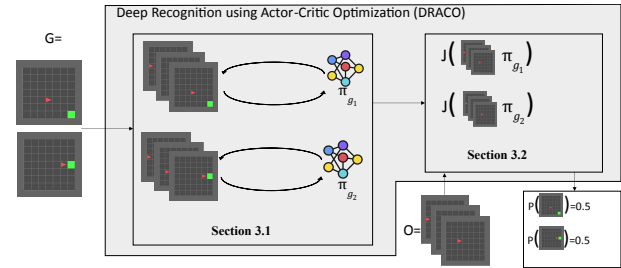


Figure 1: Overview of DRACO.

sitates a discretization process that may jeopardize recognition (Kaminka, Vered, and Agmon 2018).

This paper develops the *Deep Recognition using Actor-Critic Optimization (DRACO)* algorithm to overcome these limitations. DRACO’s input is vector-based raw data, and it outputs a distribution over the goals the observed agent might be pursuing. DRACO offers two key contributions over existing approaches to GR. First, DRACO uses interactions with the environment to learn goal-dependent neural networks (NNs), representing parameterized policies that allow us to estimate the likelihood of the observed agent pursuing each goal in virtually any type of learnable domain. Such domains include continuous domains, arbitrarily large discrete domains, and domains whose observations consist entirely of raw data. DRACO’s NNs replace the need to run costly planners in real-time, and their policies can potentially be transferred to represent new goals using transfer learning (Shamir et al. 2024; Taylor and Stone 2009). These learned policies obviate the requirement of carefully engineered domain theories and instead rely on data of the same nature as the observations we expect at recognition time. Second, this paper develops two distance measures to compare observations with the learned goal-conditioned policies, derived, respectively from Wasserstein distance, the statistical Z-score metric.

The empirical evaluation consists of two very different domains: *MiniGrid* supports discrete and continuous state space representation and a discrete action representation, while *Panda-Gym* consists of continuous state and action spaces. Each domain was evaluated on various scenarios, varied by difficulty of goal disambiguation, observability

levels, and noise level. Our comparison of DRACO with leading algorithms both in discrete and continuous environments shows that it outperforms state-of-the-art in both types of environment. In discrete domains DRACO does so even when given fewer structured inputs and fewer training episodes, whereas in continuous environments it dramatically outperforms previous approaches. Our secondary contribution is test bed for domains with continuous state and action spaces. It leverages existing RL simulations into an evaluation domain with automated instance generation.

## 2 Background

### 2.1 Recognition Problems

Goal and Activity recognition are related but distinct tasks (Van-Horenbeke and Peer 2021; Meneguzzi and Pereira 2021; Mirsky, Keren, and Geib 2021; Sukthankar et al. 2014), which have three main components. First, the *environment* specifies the problem’s dynamics and settings. Second, the *observed agent* represents the agent that acts in the environment and pursues some objective. We note that often, this *observed agent* is called an *actor*, but we use *observed agent* instead to differentiate it from the Actor in the Actor-Critic algorithm description. Third, the *observer* watches the observed agent as it acts in the environment. Beyond those similarities, each recognition problem has its own properties. *Activity Recognition* (AR) problems focus on labeling a sequence of possibly noisy sensor inputs with a single usually unstructured label, denoting a low-level activity of the observed agent, while *Goal Recognition* (GR) is the most abstract level of inference focusing on identifying the highest-level goal or overarching objective of the agent’s actions. The problem formulation in this work provides a synthesis of AR and GR, as it requires a sequence of low-level sensor data as input and outputs a prediction about the goal of the observed agent. We use a similar formulation for goal recognition as planning (Ramírez and Geffner (2009)):

**Definition 1** A *Goal Recognition (GR) problem* is a tuple  $\langle \Xi, G, O \rangle$ , such that  $\Xi$  is domain theory,  $G$  is an exhaustive and mutually exclusive set of potential goals, and  $O$  is a set of observations. A solution for a GR problem is a goal  $g \in G$  that  $O$  explains according to  $\Xi$ .

The domain theory  $\Xi$  is a description of the environment. It can be prescribed in various ways, including plan graphs (Avrahami-Zilberbrand and Kaminka 2005; E-Martín, R-Moreno, and Smith 2015), a planning domain (Ramírez and Geffner 2009; Masters and Sardina 2019; Pereira, Oren, and Meneguzzi 2020), or a Markov Decision Process (MDP) (Ramirez and Geffner 2011; Amado, Mirsky, and Meneguzzi 2022). As we combine GR and AR, such that both the goal and the observations can be either a symbolic state representation (e.g., coordinates in space), or other raw data such as images or floating point numbers vectors. Each goal  $g$  can be expressed as a formula, a set of labels over possible goal states, or a reward function over alternative sets of these states. Similarly, the observations  $O$  can be either a sequence of symbolic states or raw data. Finally, the observer can perceive all actions and state sets or only part of them.

### 2.2 Planning Domain Definition Language (PDDL)

PDDL is a formal language for describing planning problems, and introduced to standardize the representation of problems in automated planning and to serve as a common standard for benchmarking planning algorithms. A PDDL problem description typically consists of a domain file and a problem file. The domain file specifies the predicates, types, constants, and operators (actions) available, while the problem file defines the specific objects, initial state, and goal conditions.

Symbolic GR approaches relies on having a deliberate domain representation (*PDDL* for example) which is susceptible to noise, and require complete and precise specification usually made by a domain expert manually ((Ramírez and Geffner 2009; Ramírez and Geffner 2010)). This representation makes them often difficult to scale and costly in terms of real time computation.

### 2.3 Reinforcement Learning

This work focuses on Reinforcement Learning (RL)-based recognition. A commonly used domain model in RL is MDP (Sutton and Barto 2018). MDP is used to model decision-making processes, and can encapsulate both discrete and continuous state and action spaces.

**Definition 2** An *MDP*  $M$ , is a 4-tuple  $\langle S, A, P, R \rangle$  such that  $S$  are the states in the environment,  $A$  is the set of actions the agent can execute,  $P$  is a transition function, and  $R$  is a reward function. A transition function  $P(s' | s, a)$  returns the probability of transitioning from state  $s$  to state  $s'$  after taking action  $a$ , and a reward function  $R(s, a, s')$  returns the reward an agent obtains when it transitions from  $s$  to  $s'$  using action  $a$ .

The solution to an MDP is a *policy*  $\pi$ , which in RL often consists of a stochastic function  $\pi(a | s)$  that defines the probability of the agent taking action  $a \in A$  in state  $s \in S$ . A policy  $\pi_*$  is optimal if it maximizes the expected return of all states of the MDP. In Deep RL, NNs estimate these policies. In DRACO, learned policies represent the potential behavior of an observed agent rather than the desired behavior of the learner itself, and hence we can shape the reward differently for learning each goal-dependent policy.

## 3 DRACO

DRACO relies on the assumption that the environment behaves as an MDP (Definition 2) and in practice, we only need to represent states and actions as our domain theory  $\Xi$  from Definition 1:

**Definition 3** A *GR as RL problem* is a tuple  $\langle \Xi, G, O \rangle$  such that  $\Xi = \langle S, A \rangle$  is a set of  $n$ -dimensional states and  $m$ -dimensional actions, both of which can be discrete or continuous,  $S \subseteq \mathbb{R}^n$  and  $A \subseteq \mathbb{R}^m$ ;  $G \subseteq S$  is a set of potential goals, out of which we assume the observed agent pursues exactly one; and  $O = s_0, a_0, s_1, a_1, s_2, a_2, \dots$  is a sequence of state-action observations, such that  $s_i \in S$  and  $a_i \in A$ .

This definition is purposefully broad, allowing for different possible instantiations of the problem: States can be images

or continuous data such as a robot’s joints’ location and velocities. This representation obviates the need to manually prescribe labels or symbols to specific states. While we do not assume explicit transition dynamics to be part of the problem, we assume having access to the environment or some model of the environment, such as a sampling model or simulator. These assumptions free us from explicitly prescribing action dynamics as part of a recognition problem and position our solution as a model-free RL technique.

Figure 1 illustrates the recognition process in DRACO. It starts by receiving a set of goals ( $|G| = 2$  in the figure), and the observation sequence  $O$  ( $|O| = 3$  in the figure). To solve the GR problem, we first discuss how DRACO learns a set of policies, one policy for each goal, using simulated interactions. Then, we explain how DRACO compares the observation sequence  $O$  against each goal-oriented policy. Key to this comparison is the metric for processing observations and comparing them to policies. In this work, we propose two different metrics. The algorithm then outputs a distribution over the set of goals to represent how likely each goal to explain the observation.

### 3.1 Policy Learning

GR often decouples the description of the problem, including the set of recognizable goals, from a specific observation sequence (Ramirez and Geffner 2011; Masters and Sardina 2019). There is a clear gain in precomputing these policies, as the learning process is the costliest component of the pipeline, and we can assume prior knowledge of the goals in realistic domains. Consistent with this, DRACO learns a set of policies offline, one policy  $\pi_g$  for each goal  $g \in G$ . A significant strength of this approach is that it does not require the learned policies to represent agents pursuing each goal optimally. Rather, they only need to hold that a policy for goal  $g_i$  is more similar to the agent’s behavior of pursuing  $g_i$  than to the agent’s behavior of pursuing any other goal.

DRACO learns goal-dependent policies  $\pi_g$  using Actor-Critic policy gradient methods. These algorithms naturally support continuous state and action spaces, which are crucial in many physical environments, such as robotics, trajectory recognition, etc. We use the sampling model of the environment to compute the policy  $\pi_g$  for each candidate goal  $g$ . We assume our model can simulate environmental dynamics but does not contain explicit reward information. This assumption is consistent with most real-world environments, such as movement in robotic arms, which do not include explicit reward specifications. Given this model, for each goal  $g$ , DRACO generates a different reward function, meant to shape the agent’s preferences to reach that goal.

The reward function has a large influence on the learning part of the framework. Sometimes, the sparsity of the positive reward might require us to shape it further to help the agent learn how to reach the goal. Several goal-conditioned RL algorithms apply here (Andrychowicz et al. 2017; Durgkar et al. 2021; Kaelbling 1993; Schaul et al. 2015), and transfer learning techniques can be used to learn new policies for new goals quickly, thus enabling DRACO to scale quickly with the number of goals. However, to minimize variability in this work, in our empirical evaluation we re-

place these sophisticated algorithms with a simple aggregated reward. To train the goal-dependent policy  $\pi_g$ , we consider the reward for action  $a$  in state  $s$  to be:

$$R_g(s, a) = (-1) * \|a(s) - g\|_{L_1} \quad (1)$$

**Learning Architectures** This work focuses on Actor-Critic (AC) approaches to learn the goal-dependent policies since they are the leading approaches in policy-based continuous RL. Each AC algorithm requires two NNs per goal (actor NN and critic NN), so its total number of trained NNs is  $2 \times |G|$ . The Actor network outputs a probability of taking each action, the size of its output is the number of valid actions. By contrast, the critic network, which outputs the expected value for being in this particular state, has a single neuron in its last layer. Once DRACO computes these two NNs, it uses the Actor’s output to generate policies for each goal ( $\pi_g$ ) and an observation sequence  $O$  for GR: inferring the goal ( $g \in G$ ) that  $O$  explains. The reason that we chose to use the Actor network’s output rather than the Critic network’s is that the Actor network outputs an action rather than a value, which is easier to compare to the observation sequence.

### 3.2 Likelihood Estimation of Observations (inference)

Following the Bayesian formulation from Ramírez and Geffner (2010), we compute the probability  $P(g | O)$  of a goal  $g \in G$  conditioned on observations  $O$  by computing the probability  $P(O | g)$  of the observations conditioned on the goals. The key challenge here is to estimate the likelihood of  $O$  given  $g$ , which is the likelihood of taking the action  $a$  when in state  $s$  according to  $\pi_g$ . Formally,  $\pi_g(a | s) \doteq P(a | s, g)$ . For this estimation, we need to design a distance function between an observation sequence of the form  $s_0, a_0, s_1, a_1, \dots$  and a policy  $\pi_g(a_i | s_i)$ . This function should be able to handle continuous spaces to enable goal recognition in such environments. We can then compute an aggregate distance  $\Delta$  of the observations  $O$  to the observations we expect an agent to generate if it follows a policy towards that goal at each step in the observations. This metric allows us to compute the probability of the observations for each goal using the softmax of such distances:

$$P(O | g) = \text{soft} \min_{g \in G} (\Delta(O, \pi_g)) \quad (2)$$

Then, using the assumption of exhaustive and mutually exclusive goal hypotheses from Definition 1, we can compute the probability of each goal hypothesis by normalizing over the individually computed conditional probabilities in Eq. 3.

$$P(g | O) = \frac{P(O | g)P(g)}{\sum_{g_i \in G} P(O | g_i)} \quad (3)$$

We develop three functions to serve as our distance metrics to measure the difference between an observation and policy  $\pi_p$ . Since observation can be perceived in two main formats: state only list, and state and action tuples list, in this work we suggest metrics for both observations formats.

### 3.3 Observation distance functions

**Max utility for State-only**  $O^s$  applies to state-only observations and is defined by a sequence of states  $\langle s_1, \dots, s_k \rangle$ . In the AC algorithm family, the critic network estimates  $V(S)$ , the expected return from  $s$  following a particular policy  $\pi$ .  $V(s)$  expresses how good it is to be in  $s$ , and the higher  $V(s)$  the more the network thinks  $s$  promise. We take advantage of the ability of AC to estimate  $V(S)$ , and present a state-only distance based on this estimation.

$$D_s(O^s) = D_s(\langle s_1, \dots, s_k \rangle) = \frac{1}{\sum_{s_i \in O^s} V(s_i)} \quad (4)$$

In this work, as explained in Equation 2, the goal that minimizes the distance between the policy and the given observation is the goal the framework suggests the agent aims. Having said that, as the observation explains the goal better, we aim to minimize the result of distance mathematical computation.

Since in this work we use a non positive simple reward function explained in Eq 1, as the  $V(s_k \in O^s)$  becomes smaller (meaning that the state is less attractive), the state-only distance (Eq 4) becomes larger and vice versa. If an observation contains more promising goals, their  $\sum_{s_k \in O^s} V(s_k)$  will be larger causing  $D_s(O^s)$  to become lower (sum of non positives) and eventually be assessed as a more promising goal candidate.

**Wasserstein distance** computes the amount of work to convert one distribution to another (Vallender 1974).

$$W_p(P, Q) = \frac{1}{k} \sum_{i=1}^k \|X_i - Y_i\|_{L_1} \quad (5)$$

Eq. 5 encodes the Wasserstein distance measure for one-dimensional distributions, with 1 statistical moment, for two empirical distributions  $P$  and  $Q$  with samples  $X_1, \dots, X_k$  and  $Y_1, \dots, Y_k$  respectively. We adapt this equation to compute the spot Wasserstein distance between an observation  $o = s, a$  and a goal-dependent policy  $\pi$ , from which we sample actions  $\tilde{a}$  (denoted by  $\tilde{\pi}(s)$ ):

$$W_p(s, a, \pi) = \|a - (\tilde{a} \sim \pi(s))\|_{L_1} \quad (6)$$

As this score looks at a single observation at a time, we omit the sum over  $n$  samples. Finally, we compute the Wasserstein distance between the observation sequence and the goal-dependent policy.

$$\Delta_{W_p}(O, \pi) = \mu(\{w_i \mid w_i = W_p(s_i, a_i, \pi) \forall s_i, a_i \in O\}) \quad (7)$$

**Z-score function** is a statistical measure that computes, for a value  $x$  sampled from a population, the number of standard deviations  $\sigma$  from the statistical means  $\mu$  so that  $Z(x) = (x - \mu)/\sigma$ . As seen in Figure 2, this computation is exactly what the inference process is looking for: how likely a sample (an observed action) is under some distribution (the goal-based policy). Recall that policies, by default, learned via the AC methods encodes a Gaussian distribution. Out of this Gaussian distribution, we can extract descriptive

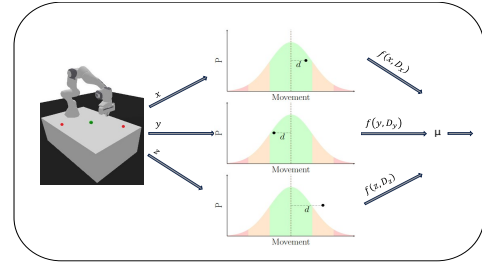


Figure 2: Z-score-based computation process: (i) input extraction; (ii) separately, calculate the Z-score of the agent’s movement and the observation. (iii), return the average of calculated Z-scores.

statistics, regardless of whether the action space is continuous or discrete, and leverage it to compute z-score. Specifically, Eq. 8 encodes the spot z-score of a single observation of state  $s$ , and action  $a$  against the action expected of policy  $\pi$  for the same state.

$$Z(s, a, \pi) = \left| \frac{a - \mu(\pi(s))}{\sigma(\pi(s))} \right| \quad (8)$$

Here  $\mu$ , and  $\sigma$  refer, respectively, to the mean and standard deviation of the numeric representation of the actions applicable in state  $s$ . We compute the distance for an entire observation sequence by taking the mean of the spot Z-scores:

$$\Delta_Z(O, \pi) = \mu(\{z_i \mid z_i = Z(s_i, a_i, \pi) \forall s_i, a_i \in O\}) \quad (9)$$

## 4 Empirical Setup and Testbed

We evaluate DRACO in two OpenAI-Gym (Brockman et al. 2016) based setups: MiniGrid (Chevalier-Boisvert et al. 2023), and Panda-gym (Gallouédéc et al. 2021). As DRACO supports both discrete and continuous setups, we compare its performance with leading state-of-the-art approaches suited for these environmental setups. For each domain, we generate GR problems by creating configurations within a shared initial setup and obstacle placement.

**Baselines.** (1) Plan Recognition as Planning: Ramirez and Geffner (R&G) is the standard baseline for symbolic GR and leverage planner executions for GR (Ramirez and Geffner 2011). Since it relies on a PDDL domain representation that is either manually crafted (Vered and Kaminka 2017) or generated from labelled data (Granada et al. 2020), it cannot be trivially used in continuous domains, so we use it for evaluating MiniGrid. (2) GRAQL (Amado, Mirsky, and Meneguzzi 2022) learns a Q-table per goal and uses them to compute the likelihood of each goal hypothesis. GRAQL’s tabular nature limits it to discrete domains, so we discretize domains to compare it with DRACO in continuous setups.

**Algorithms.** In this evaluation, DRACO learns policies via Proximal Policy Optimization (PPO) (Schulman et al. 2017), from Stable Baselines (Raffin et al. 2021) and infers using of Z-score and Wasserstein distance function metrics proposed in section 3.3. GRAQL and DRACO require offline domain’s learning, whereas R&G doesn’t require training,

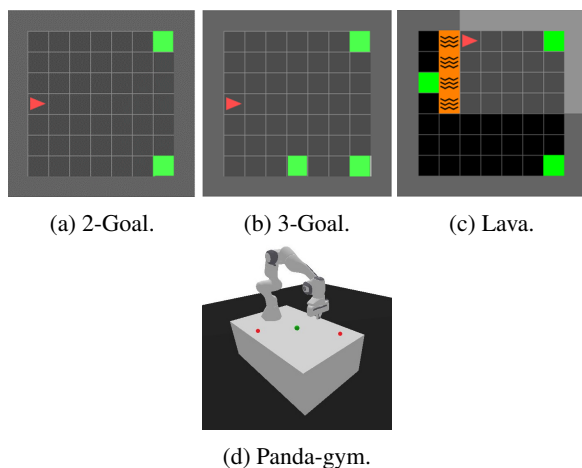


Figure 3: Example for domain setups used in evaluation.

but need to execute a planner in inference time. This implementation exemplifies how DRACO performs with an off-the-shelf DRL algorithm. GRAQL uses KL-divergence for inference in MiniGrid, but its performance in discretized-continuous environments is often poor because of the high number of actions, which makes the probability that the observation and the policy converge on the same action infeasible. To address it, in the discretized environments, we use the mean of the action distances to the observation instead.

**Hyperparameters.** While GRAQL and DRACO use different training algorithms, they share various hyperparameters, such as number of episodes, learning rate, and discount factor. Throughout the executions, optimizing the approach’s performance was the leading motivation. We used the hyperparameter values that maximized each approach. In MiniGrid, we compare GRAQL and DRACO after 100K episodes, discount factor ( $\gamma$ ) 0.99, and learning rate ( $\alpha$ ) 0.001. In Panda-Gym, we tracked the learning’s performance under multiple episode configurations until convergence. The optimal discretization factor for GRAQL is 0.03 cm. Similarly, in Panda-Gym, GRAQL’s learning rate ( $\gamma$ ) was 0.01 while DRACO’s was 0.0006. For R&G, we created a PDDL-based domain theory using PDDL-generator (Seipp, Torralba, and Hoffmann 2022).

**Metrics.** We leverage standard prediction metrics from machine learning, to the context of goal recognition, to “correctly classify” the true goal means it has the highest probability. As such, the meaning of these metrics for GR is as follows: Accuracy and precision measure how often a method correctly classifies the correct and incorrect goals, respectively, and recall measures how often a method identifies the correct goal as the most likely. Finally, we evaluate the framework’s confidence in its prediction. The confidence metric is the difference between the probabilities of the two most probable goals divided by the most probable goal’s probability. Thus, if two (or more) most likely goals are *equiprobable*, confidence is *zero*.

**Domain 1: MiniGrid.** The motivation to use MiniGrid is the ability to be represented in multiple formats and to

Domain	Problem	WCD	WCD / $-\ p_g\ $	Domain	Problem	WCD ( $\delta = 0.01cm$ )	W
MiniGrid	Lava	5	5/11 $\approx$ 45%	Panda-Gym	2-Goals	1	
	2-Goals	6	6/9 $\approx$ 66%		3-Goals	4	
	3-Goals	6	6/9 $\approx$ 66%		4-Goals	7	

Table 1: WCD metric for evaluated domains and problems.  $p_g$  is an optimal plan for a goal  $g$ .  $\delta$  is size of the perimeter we consider states to be the same (for continuous environments).

model complex GR problems. We created three environment formats, one for each algorithm: PDDLs for R&G (complete environment model), symbolic state representation for GRAQL (x and y coordinates, angle) and a visual representation for DRACO (image), making it possible to compare the different approaches in the same GR problem. Note that each representation varies in the information each algorithm perceives. MiniGrid problem consists of an agent and objective which are the red triangle and the bright green cells in Figure 3 respectively. The agent’s task is to reach the objective by taking actions: *turn right*, *turn left*, *move forward*, *do nothing*. We evaluate the three approaches on the setups depicted in Figures 3a, 3b, 3c: 2-Goal and 3-Goal are obstacle-free environments, and Lava has 3 goal candidates and lava cells. For each setup, we generated 10 different GR settings.

**Domain 2: Panda-gym** Panda-gym is a drastically different domain than MiniGrid: it has continuous state and action spaces, and it realistically presents a Franka Emika Panda robot arm (Gallouédec et al. 2021) using the PyBullet physics engine. This domain allows us to test DRACO’s boundaries and performance on a continuous state space that is not an image. This environment consists of a single arm with the objective of reaching a colored sphere (Figure 3d). Since this environment is fully continuous and does not inherently support discrete state spaces, we provide a discretization of the environment in order to run the GRAQL baseline on it. Specifically, we tested discretization granularities of 0.01 – 0.05 cm and eventually chose 0.03 cm as this value yields the best performance for our GRAQL baseline. To stress out approach, we ran both DRACO and GRAQL on three different GR setups, with 2,3, and 4 goal spheres (Figure 3d illustrates Panda-Gym 3-goals problem). For each setup, we generated 10 different GR settings.

**Domain ambiguity** We assess the level of domain ambiguity using the *worst-case distinctiveness (WCD)* metric (Keren, Gal, and Karpas 2014). WCD represents the maximum steps an optimal agent can take before an *observer* can differentiate the correct goal. Since WCD accounts only for discrete states, in Panda-gym, we consider all states in a perimeter of 0.01 cm around a state to be the same. Table 1 summarizes the WCD on evaluated domains, and shows that across all domains, we specifically chose ambiguous setups in which it would be challenging to perform GR. Notably, in Panda-Gym 3 and 4 goals and in MiniGrid 2 and 3 goals problems, the movements towards the goal under some partial observability conditions (mainly 10% and 30%) can even be impossible to disambiguate.

OBS	Problem	DRACO using KL-Divergence					GRAQL using KL-Divergence					Ramirez and Geffner				
		Accuracy	Precision	Recall	F-Score	Conf.	Accuracy	Precision	Recall	F-Score	Conf.	Accuracy	Precision	Recall	F-Score	Conf.
10%	Lava	0.73 ± 0.32	0.6 ± 0.52	0.6 ± 0.52	0.6 ± 0.52	<b>81%</b>	0.53 ± 0.32	0.41 ± 0.36	0.9 ± 0.32	0.56 ± 0.32	5%	<b>1.0 ± 0.0</b>	<b>0.77 ± 0.46</b>	<b>1.0 ± 0.0</b>	<b>0.87 ± 0.46</b>	70%
	2-Goals	<b>1.0 ± 0.0</b>	<b>1.0 ± 0.0</b>	<b>1.0 ± 0.0</b>	<b>1.0 ± 0.0</b>	<b>77%</b>	0.70 ± 0.35	0.64 ± 0.35	0.9 ± 0.31	0.75 ± 0.32	13%	<b>1.0 ± 0.0</b>	0.5 ± 0.0	<b>1.0 ± 0.0</b>	0.67 ± 0.00	0%
	3-Goals	<b>1.0 ± 0.0</b>	<b>1.0 ± 0.0</b>	<b>1.0 ± 0.0</b>	<b>1.0 ± 0.0</b>	<b>78%</b>	0.66 ± 0.35	0.56 ± 0.40	0.9 ± 0.32	0.64 ± 0.35	6%	<b>1.0 ± 0.0</b>	0.36 ± 0.0	<b>1.0 ± 0.0</b>	0.52 ± 0.00	0%
30%	Lava	0.93 ± 0.21	0.9 ± 0.31	0.9 ± 0.31	0.9 ± 0.31	<b>64%</b>	0.87 ± 0.28	0.80 ± 0.42	0.80 ± 0.42	0.80 ± 0.42	8%	<b>1.0 ± 0.0</b>	<b>1.0 ± 0.0</b>	<b>1.0 ± 0.0</b>	<b>1.0 ± 0.0</b>	55%
	2-Goals	<b>1.0 ± 0.0</b>	<b>1.0 ± 0.0</b>	<b>1.0 ± 0.0</b>	<b>1.0 ± 0.0</b>	<b>65%</b>	<b>1.0 ± 0.0</b>	<b>1.0 ± 0.0</b>	<b>1.0 ± 0.0</b>	<b>1.0 ± 0.0</b>	12%	<b>1.0 ± 0.0</b>	0.71 ± 0.49	<b>1.0 ± 0.0</b>	0.83 ± 0.48	30%
	3-Goals	<b>1.0 ± 0.0</b>	<b>1.0 ± 0.0</b>	<b>1.0 ± 0.0</b>	<b>1.0 ± 0.0</b>	<b>38%</b>	<b>1.0 ± 0.0</b>	<b>1.0 ± 0.0</b>	<b>1.0 ± 0.0</b>	<b>1.0 ± 0.0</b>	11%	<b>1.0 ± 0.0</b>	0.62 ± 0.49	<b>1.0 ± 0.0</b>	0.77 ± 0.48	30%

Table 2: The table reports the average performance ( $\pm$  standard deviation) of the algorithms over 30 different GR settings under 10% and 30% partial observability. *Conf.* stands for Confidence

## 5 Results

Our tests use a different algorithm from our learning methods to generate observations, namely Asynchronous Actor-Critic (A2C) (Mnih et al. 2016). For each combination of algorithm and instance, the observation sequence  $O$  varies its degree of observability: 10%, 30%, 50%, 70%, and full observability. We generate an observation sequence with  $x\%$  observability by taking a full sequence and removing each observation along the trajectory with  $x\%$  probability. Similarly, we generate noisy observations by appending suboptimal actions to  $x\%$  of the states.<sup>1</sup> For each execution in every environment, we use the same trajectories for all algorithms. We show the metrics averaged over 10 settings with varying degrees of observability (13 configurations per execution), totalling 540 GR problem instances.

**Performance** Table 2 shows results for MiniGrid. All approaches perform overwhelmingly well, with perfect scores on all measures when the observability is 0.5 or higher. However, this result misses part of the story: while GRAQL’s and R&G’s true goal confidence score was close to the other goals’ score (9% and 13% difference on average respectively), DRACO had very different scores between the true goal and the other candidates (71% on average), making DRACO more confident in its predictions. Moreover, DRACO’s results dominate GRAQL’s and R&G results in the more challenging, low observability (10%, 30%), problem variants. It is a reasonable outcome because DL can make significant inroads to recognizing patterns and variance instead of valuing the current state. Moreover, our use of NN-based policies makes DRACO more forgiving to missing observations, as the likelihood of these missing actions is  $\epsilon$  rather than zero, and this difference is accumulated with the number of missing observations. Lastly, as this table shows, DRACO and GRAQL both outperform the R&G approach in most of these discrete domains. Importantly, DRACO dominates both approaches in the confidence metric, inferring higher probabilities for the correct goal, whereas GRAQL and R&G often disambiguate poorly. Note that the accuracy metric in this paper differs from Ramirez and Geffner (2010), which refers to the ratio of problems where the recognizer ranks the true goal (i.e., True Positives) with the highest likelihood, and the number of problems tested. This measure differs from standard ML accuracy, which also factors in the successful ranking of the correct goal (i.e., True Positives + True Negatives). In our experiments, we report accuracy using the latter definition.

Figure 4 reports the average F-Score for all Panda-Gym

problems running GRAQL in a discretized environment version and DRACO in the continuous environment representation, both with the Z-score and the Wasserstein distance metrics. Figure 4a shows the mean performance with full observability, and Figures 4b- 4c show the mean performance under partial and noisy observations. First, DRACO’s performance is similar and often superior to GRAQL, often reaching the best results regardless of the distance metric used. GRAQL struggles in generalizing continuous and relatively large environments. This gap happens due to one of the main differences between DL and tabular methods — DL approximates states similar to visited ones while Q-Learning does not, affecting the number of episodes GRAQL requires to learn how to solve a problem. Figures 4a and 4b compare the approaches under increasing episodes and observability percentage, respectively.<sup>2</sup> These figures emphasize the superiority of DRACO over GRAQL across the board in continuous environments. GRAQL performance improves when episodes increase but generalizing a large problem for GRAQL takes a substantially more amount of computations than it takes for DRACO. However, in the partial observation scenario (Figure 4b), as the observability percentage increases DRACO’s performance increases as well while GRAQL’s remains about the same, thus emphasizing its inability to learn the problem (even for the 100% observability problem). Figure 4c illustrates performance under noisy (but complete) observations. DRACO outperforms GRAQL with low variance, showing its substantial resilience to noise. DRACO was barely impacted by the 10% and 20% noise ratio, preserving its performance from the full-observable non-noisy observation. Indeed, the gap between DRACO and GRAQL increases as the noise ratio decreases. Such a difference in performance is again likely due to its leverage of DL to the learning stage and the richer representation state available to DRACO. Additionally, Figure 4 also compares the different distance metrics proposed in this paper in section 3.2. Figure 4a shows a slight dominance of DRACO using Wasserstein distance over DRACO using Z-score when trained for  $< 125K$  but for 150K+ episodes, this trend changes. The number of trained episodes impacts the agent’s optimality, making the Z-score metric better for scenarios where the trained agent policy is more optimal. This behavior happens because the Z-score metric takes into consideration the standard deviation of the policy distribution which takes more episodes to stabilize. Figures 4b, 4c shows a dominance of Wasserstein over Z-score, for observability levels of  $< 50\%$  and with noisy observations. Wasserstein

<sup>1</sup>Examples of noisy observations in the supplement.

<sup>2</sup>Supplementary material includes a breakdown of the results.

is better under high uncertainty stemming from the observations, as the Z-score metric is more sensitive to high variability that skews it from the right goal.

**Scalability.** Scalability evaluation has three main factors: storage, training, and execution time. First, in terms of storage consumption, DRACO uses a constant  $8 \pm 0$  MB while GRAQL  $3190 \pm 700$  MB. This difference is primarily due to the huge storage needs of the Q-table used by GRAQL. By contrast, DRACO uses constant memory because it stores only the network architecture and neurons’ values. Even though these neurons’ values change along the training time, their memory consumption remains constant. Second, DRACO’s average training time was  $13.52 \pm 4.3$  minutes while GRAQL’s was  $1108 \pm 463$  minutes. We trained both approaches on the same commodity Tesla K40 server. This difference is due to two factors: (1) GRAQL relies on the CPU for its computation, whereas DRACO uses a GPU; and (2) GRAQL’s storage-intensive operations are more expensive. Notably, R&G does not require training time, yet its on-line time is significantly higher than the other algorithms, as it runs planners in inference time. Specifically, DRACO and GRAQL’s online runtime takes  $\approx 0.12$  and  $\approx 0.1$  seconds on average respectively while R&G takes  $\approx 2$  seconds. Third, as discussed in section 3.2, GRAQL and DRACO load their policies before inference. GRAQL’s Q-tables loading time is often not negligible and takes an average of  $\approx 3.4$  minutes per table while DRACO’s NNs loading takes seconds.

To conclude, we evaluate the paper’s two main contributions: the DRACO framework and the proposed distance metrics. DRACO scaled better than the state-of-the-art GR algorithms in storage consumption, computation time, and performance. DRACO requires no domain expert to craft an elaborate model like R&G and instead learns via interactions. It achieves better or equal performance results compared to GRAQL and R&G, with both metrics performing overwhelmingly well. Wasserstein was slightly better in less observable spaces and under noisy observations.

## 6 Related Work

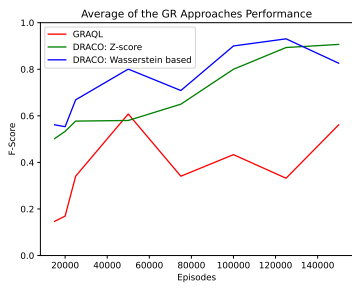
Goal recognition research can be categorized into two main categories: symbolic and data-driven GR. Symbolic approaches leverage planning, search, and parsing techniques to infer which goal best explains a sequence of symbols (Geib and Goldman 2009; Pereira, Oren, and Meneguzzi 2020). These approaches heavily rely on a domain expert to provide a problem and environment formulation, which makes them difficult to scale and susceptible to noise. By contrast, data-driven GR obviates or mitigates the need for a domain expert. Some learning-based approaches rely on process mining techniques (Polyvyanyy et al. 2020; Ko et al. 2023). These approaches compare an observation sequence to past traces, which makes them brittle when handling large or continuous action spaces. Recent work lifts the requirement of domain experts by relying on tabular RL or DL (Zeng et al. 2018; Min et al. 2014). Amado, Mirsky, and Meneguzzi (2022) develop a GR approach based on tabular RL techniques to learn the domain model, and Fang et al. (2023) extend this work to robotics simulators. Like many other RL algorithms, these algorithms assume that the

agent’s environment is an MDP. Both Chiari et al. (2022) and Maynard, Duhamel, and Kabanza (2019) use DL to solve GR problems. They propose neural network (NN) architectures that get observations as input and return the probability of reaching each goal. Although the DL approaches presented in these papers present major improvements, it also faces several difficulties. Chiari et al. (2022) discretises the continuous environment and hence suffers from the same discretisation issues discussed earlier. Maynard, Duhamel, and Kabanza (2019) mitigate this by working directly with images of the domain. These approaches require extensive data collection, making them highly inflexible to changes and previously unseen states. DRACO provides a compromise between these approaches: it uses unstructured input, but a distinct NN is allocated for each potential goal, so learning is focused and efficient. DRACO can recognize goals within all the available fluents of the domain as long as interacting with the environment (or a simulation) is possible, which is often a limitation in machine learning approaches for GR (Zhuo et al. 2020).

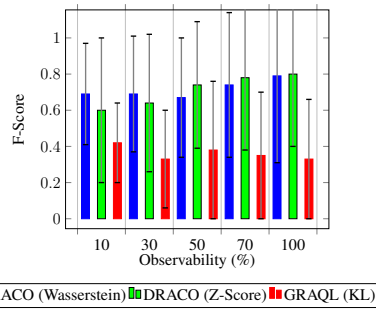
## 7 Conclusion

This paper provides a novel approach for end-to-end goal recognition in continuous domains. Its contributions include the DRACO algorithm, two distance metrics to compare observed trajectories to a policy, and a testbed of unstructured goal recognition environments and various problems. DRACO is shown to be more accurate, have higher confidence, and scale better than existing approaches, both in discrete and continuous domains. DRACO has many advantages over symbolic and tabular RL approaches. First, it works in both continuous and discrete domains without having the recognition process affected by the quality of a training set. Such approaches are limited by the states and goals within the dataset. Second, its memory footprint and sample efficiency scale better, as earlier algorithms depend on the size of the state and action spaces. Third, it doesn’t require a domain-expert to provide the problem’s formulation. Finally, value-based RL techniques like Q-learning often fail in continuous domains due to instability and poor convergence, leading to suboptimal policies.

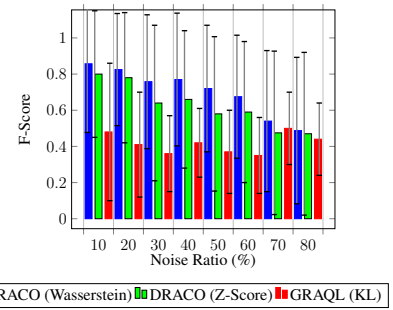
While DRACO is promising for robust goal recognition, it has three limitations: First, access to simulations: DRACO requires executing multiple instances to learn the goal-dependent policies. While this does not require DRACO to perfectly replicate the actor’s policy, it should be able to produce policies that are different enough from one another. In the future, we aim to extend our work to use policies learned from Imitation Learning (Hussein et al. 2017) or Learning from Observation (Zhu et al. 2020) techniques. Second, number of goals: While DRACO’s online inference is fast, it still needs to learn a new policy for each goal the actor might pursue. Potential ways to overcome this are using universal value functions (Schaul et al. 2015) or transfer learning techniques (Taylor and Stone 2009). Third, learning quality: More complex domains may require elaborate learning techniques. DRACO’s PPO can be replaced by more sophisticated RL algorithms. For example, image-processing techniques (Gedraite and Hadad 2011) or policy acquisition



(a) Performance with varying episodes



(b) Performance with varying degrees of observability.



(c) Performance with noisy observations across all domains.

Figure 4: Panda-gym domain results of F-score for GRAQL, DRACO with Z-score, and DRACO with Wasserstein, observability (a), and noise (b). Error bars indicate standard deviation.

techniques such as inverse RL (Ng, Russell et al. 2000) can fine-tune the policies. DRACO provides a consistent infrastructure through which such solutions can be implemented.

## References

- Amado, L.; Mirsky, R.; and Meneguzzi, F. 2022. Goal recognition as reinforcement learning. In *Proceedings of the AAAI Conference on Artificial Intelligence*, volume 36, 9644–9651.
- Andrychowicz, M.; Wolski, F.; Ray, A.; Schneider, J.; Fong, R.; Welinder, P.; McGrew, B.; Tobin, J.; Pieter Abbeel, O.; and Zaremba, W. 2017. Hindsight experience replay. *Advances in neural information processing systems*, 30.
- Avrahami-Zilberbrand, D.; and Kaminka, G. A. 2005. Fast and Complete Symbolic Plan Recognition. In *IJCAI*, 653–658.
- Brockman, G.; Cheung, V.; Pettersson, L.; Schneider, J.; Schulman, J.; Tang, J.; and Zaremba, W. 2016. Openai gym. *arXiv preprint arXiv:1606.01540*.
- Chevalier-Boisvert, M.; Dai, B.; Towers, M.; de Lazcano, R.; Willems, L.; Lahlou, S.; Pal, S.; Castro, P. S.; and Terry, J. 2023. Minigrid & Miniworld: Modular & Customizable Reinforcement Learning Environments for Goal-Oriented Tasks. *CoRR*, abs/2306.13831.
- Chiari, M.; Gerevini, A. E.; Putelli, L.; Percassi, F.; and Serina, I. 2022. Goal Recognition as a Deep Learning Task: the GRNet Approach. *arXiv preprint arXiv:2210.02377*.
- Durugkar, I.; Tec, M.; Niekum, S.; and Stone, P. 2021. Adversarial intrinsic motivation for reinforcement learning. *Advances in Neural Information Processing Systems*, 34: 8622–8636.
- E-Martín, Y.; R-Moreno, M. D.; and Smith, D. E. 2015. A fast goal recognition technique based on interaction estimates. In *Proceedings of the 24th International Conference on Artificial Intelligence*, 761–768.
- Fang, Z.; Chen, D.; Zeng, Y.; Wang, T.; and Xu, K. 2023. Real-Time Online Goal Recognition in Continuous Domains via Deep Reinforcement Learning. *Entropy*, 25(10): 1415.
- Gallouédec, Q.; Cazin, N.; Dellandréa, E.; and Chen, L. 2021. panda-gym: Open-Source Goal-Conditioned Environments for Robotic Learning. *4th Robot Learning Workshop: Self-Supervised and Lifelong Learning at NeurIPS*.
- Gedraite, E. S.; and Hadad, M. 2011. Investigation on the effect of a Gaussian Blur in image filtering and segmentation. In *Proceedings ELMAR-2011*, 393–396. IEEE.
- Geib, C. W.; and Goldman, R. P. 2009. A probabilistic plan recognition algorithm based on plan tree grammars. *Artificial Intelligence*, 173(11): 1101–1132.
- Granada, R.; Monteiro, J.; Gavenski, N.; and Meneguzzi, F. 2020. Object-based goal recognition using real-world data. In *Mexican International Conference on Artificial Intelligence*, 325–337. Springer.
- Hussein, A.; Gaber, M. M.; Elyan, E.; and Jayne, C. 2017. Imitation Learning: A Survey of Learning Methods. *ACM Computing Surveys*, 50(2): 21:1–21:35.
- Kaelbling, L. P. 1993. Learning to achieve goals. In *IJCAI*, volume 2, 1094–8. Citeseer.
- Kaminka, G.; Vered, M.; and Agmon, N. 2018. Plan recognition in continuous domains. In *Proceedings of the AAAI Conference on Artificial Intelligence*, volume 32.
- Kautz, H. A.; Allen, J. F.; et al. 1986. Generalized plan recognition. In *AAAI*, volume 86, 5. Philadelphia, PA.
- Keren, S.; Gal, A.; and Karpas, E. 2014. Goal recognition design. In *Twenty-Fourth International Conference on Automated Planning and Scheduling*.
- Ko, J.; Maggi, F. M.; Montali, M.; Peñalosa, R.; and Pereira, R. F. 2023. Plan Recognition as Probabilistic Trace Alignment. In *5th International Conference on Process Mining (ICPM)*.
- Masters, P.; and Sardina, S. 2019. Cost-based goal recognition in navigational domains. *Journal of Artificial Intelligence Research*, 64: 197–242.
- Maynard, M.; Duhamel, T.; and Kabanza, F. 2019. Cost-based goal recognition meets deep learning. *arXiv preprint arXiv:1911.10074*.



- Meneguzzi, F.; and Pereira, R. F. 2021. A survey on goal recognition as planning. In *Proceedings of the 30th International Joint Conference on Artificial Intelligence (IJCAI), 2021, Canada*.
- Min, W.; Ha, E.; Rowe, J.; Mott, B.; and Lester, J. 2014. Deep learning-based goal recognition in open-ended digital games. In *Proceedings of the AAAI Conference on Artificial Intelligence and Interactive Digital Entertainment*, volume 10, 37–43.
- Mirsky, R.; Keren, S.; and Geib, C. 2021. Introduction to symbolic plan and goal recognition. *Synthesis Lectures on Artificial Intelligence and Machine Learning*, 16: 1–190.
- Mnih, V.; Badia, A. P.; Mirza, M.; Graves, A.; Lillicrap, T.; Harley, T.; Silver, D.; and Kavukcuoglu, K. 2016. Asynchronous methods for deep reinforcement learning. In *International conference on machine learning*, 1928–1937. PMLR.
- Ng, A. Y.; Russell, S. J.; et al. 2000. Algorithms for inverse reinforcement learning. In *Icml*, volume 1, 2.
- Pereira, R. F.; Oren, N.; and Meneguzzi, F. 2020. Landmark-based approaches for goal recognition as planning. *Artificial Intelligence*, 279: 103217.
- Polyvyanyy, A.; Su, Z.; Lipovetzky, N.; and Sardina, S. 2020. Goal Recognition Using Off-The-Shelf Process Mining Techniques. In *AAMAS*, 1072–1080.
- Qin, X.; and Lee, W. 2004. Attack plan recognition and prediction using causal networks. In *20th Annual Computer Security Applications Conference*, 370–379. IEEE.
- Raffin, A.; Hill, A.; Gleave, A.; Kanervisto, A.; Ernestus, M.; and Dormann, N. 2021. Stable-baselines3: Reliable reinforcement learning implementations. *The Journal of Machine Learning Research*, 22(1): 12348–12355.
- Ramírez, M.; and Geffner, H. 2009. Plan recognition as planning. In *Twenty-First international joint conference on artificial intelligence*.
- Ramirez, M.; and Geffner, H. 2011. Goal recognition over POMDPs: Inferring the intention of a POMDP agent. In *Twenty-second international joint conference on artificial intelligence*.
- Ramírez, M.; and Geffner, H. 2010. Probabilistic Plan Recognition Using Off-the-Shelf Classical Planners. In *AAAI Conference on Artificial Intelligence*.
- Schaul, T.; Horgan, D.; Gregor, K.; and Silver, D. 2015. Universal value function approximators. In *International conference on machine learning*, 1312–1320. PMLR.
- Schulman, J.; Wolski, F.; Dhariwal, P.; Radford, A.; and Klimov, O. 2017. Proximal policy optimization algorithms. *arXiv preprint arXiv:1707.06347*.
- Seipp, J.; Torralba, Á.; and Hoffmann, J. 2022. PDDL Generators. <https://doi.org/10.5281/zenodo.6382173>.
- Shamir, M.; Elhadad, O.; Taylor, M. E.; and Mirsky, R. 2024. ODGR: Online Dynamic Goal Recognition. In *Finding the Frame: An RLC Workshop for Examining Conceptual Frameworks*.
- Shvo, M.; Hari, R.; O’Reilly, Z.; Abolore, S.; Wang, S.-Y. N.; and McIlraith, S. A. 2022. Proactive Robotic Assistance via Theory of Mind. In *2022 IEEE/RSJ International Conference on Intelligent Robots and Systems (IROS)*, 9148–9155. IEEE.
- Sukthankar, G.; Geib, C.; Bui, H.; Pynadath, D.; and Goldman, R. P. 2014. *Plan, activity, and intent recognition: Theory and practice*. Newnes.
- Sutton, R. S.; and Barto, A. G. 2018. *Reinforcement learning: An introduction*. MIT press.
- Taylor, M. E.; and Stone, P. 2009. Transfer learning for reinforcement learning domains: A survey. *Journal of Machine Learning Research*, 10(7).
- Vallender, S. 1974. Calculation of the Wasserstein distance between probability distributions on the line. *Theory of Probability & Its Applications*, 18(4): 784–786.
- Van-Horenbeke, F. A.; and Peer, A. 2021. Activity, plan, and goal recognition: A review. *Frontiers in Robotics and AI*, 8: 643010.
- Vered, M.; and Kaminka, G. A. 2017. Online recognition of navigation goals through goal mirroring. In *Proceedings of the 16th Conference on Autonomous Agents and Multiagent Systems*, 1748–1750.
- Zeng, Y.; Xu, K.; Yin, Q.; Qin, L.; Zha, Y.; and Yeoh, W. 2018. Inverse Reinforcement Learning Based Human Behavior Modeling for Goal Recognition in Dynamic Local Network Interdiction. In *The Workshops of the The Thirty-Second AAAI Conference on Artificial Intelligence*, 646–653.
- Zhu, Z.; Lin, K.; Dai, B.; and Zhou, J. 2020. Off-policy imitation learning from observations. *Advances in Neural Information Processing Systems*, 33: 12402–12413.
- Zhuo, H. H.; Zha, Y.; Kambhampati, S.; and Tian, X. 2020. Discovering Underlying Plans Based on Shallow Models. *ACM Transactions on Intelligent Systems and Technology*, 11(2).